International Journal of Biological Macromolecules 120 (2018) 45–58

Contents lists available at ScienceDirect

International Journal of Biological Macromolecules

journal homepage: http://www.elsevier.com/locate/ijbiomac

Rutin attenuates negatively charged surfactant (SDS)-induced lysozyme aggregation/amyloid formation and its cytotoxicity

Mohd Shahnawaz Khan [a,*], Sheraz Ahmad Bhat [b], Md Tabish Rehman [c], Iftekhar Hassan [d], Shams Tabrez [e], Mohamed F. AlAjmi [c], Afzal Hussain [c], Fohad Mabood Husain [f], Salman Freeh Alamery [g]

[a] Protein Research Chair, Department of Biochemistry, College of Science, King Saud University, Riyadh 11451, Saudi Arabia
[b] Department of Biochemistry, Govt. Degree College, Kashmir University, Jammu and Kashmir, India
[c] Department of Pharmacognosy, College of Pharmacy, King Saud University, Riyadh 11451, Saudi Arabia
[d] Department of Zoology, College of Science, King Saud University, Riyadh 11451, Saudi Arabia
[e] King Fahad Medical Research Center, King Abdulaziz University, P.O. Box 80216, Jeddah 21589, Saudi Arabia
[f] Department of Agriculture and Food Chemistry, King Saud University, Riyadh 11451, Saudi Arabia
[g] Center of Excellence in Biotechnology Research, Dept. Of Biochemistry, College of Science, King Saud University, Saudi Arabia

ARTICLE INFO

Article history:
Received 14 February 2018
Received in revised form 11 July 2018
Accepted 17 July 2018
Available online 04 August 2018

Keywords:
Amyloid
Lysozyme
SDS
Rutin
Cytotoxcity
Genotoxcity
Docking

ABSTRACT

Amyloid fibrils are highly ordered protein assemblies known to contribute to the pathology of a variety of genetic and aging-associated diseases. Here, we have investigated the aggregation propensity of lysozyme in the presence of a negatively charged surfactant (SDS) and evaluated the anti-aggregation activity of rutin. Multiple approaches such as turbidity measurements, dye binding assays, intrinsic fluorescence, circular dichroism (CD), transmission electron microscopy (TEM), MTT and comet assays have been used for this purpose. We inferred that SDS induces aggregation of lysozyme in 0.2–0.6 mM concentration range while at higher concentration range (0.8–1.0 mM), it leads to solubilization/stabilization of protein. Intrinsic/extrinsic fluorescence and CD analysis confirmed significant conformational changes in lysozyme at 0.2 mM SDS. Thioflavin T (ThT), congo red binding and TEM analysis further reaffirmed the formation of lysozyme fibrils. Moreover, MTT assay demonstrated cytotoxicity of these fibrils towards neuroblastoma cell lines (SH-SY5Y) and their attenuation by rutin. Comet assay supported the cytotoxicity mechanism *via* DNA damage. Molecular docking results also advocate a strong interaction between lysozyme and rutin. The current study indicates a mechanistic approach assuming structural constraints and specific aromatic interactions of rutin with HEWL aggregates.

1. Introduction

Protein amyloid aggregation has received extensive attention in biology, medicine, and biophysics because of its implication in several human diseases [1]. Amyloid aggregates are insoluble protein aggregates with the characteristic cross-β structure and fibrous morphology [2]. Deposition of amyloid aggregate in tissues is a pathological hallmark of >40 neurodegenerative, systemic, and nonsystemic diseases which apart from others include some degenerative disorders such as chronic and progressive Alzheimer's, Parkinson's and Huntington's diseases or diabetes mellitus [3]. Several studies have shown that aggregation of proteins can be induced *in vitro* by conditions that favor partially folded or molten globule (MG)-like states [4]. Proteins, despite their unrelated amino acid sequences and tertiary structures, can unfold and assemble into fibrils with similar ultra-structures and identical biochemical properties. Protein aggregates are characterized by long and unbranched fibrils with enriched β-sheet structure, increased surface hydrophobicity, fluorescence upon binding to thioflavin T (ThT) and the ability to disrupt cellular membranes [5]. Inhibition of amyloid fibrils thus opens up a scope for the treatment of neurological disorders which involves either preventing the proteins to undergo self-association or disintegration of mature fibrils.

Hen egg-white lysozyme (HEWL), a 129-residue monomeric globular protein with molecular weight of 14.3 kD, has been extensively used as a food preservative owing to its lytic activity against the cell wall of Gram-positive bacteria [6,7]. Structurally, HEWL, in its native conformation, is a helix-rich protein (α-helix: ~30%) containing two different domains which are cross-linked using four disulfide bonds [8,9]. HEWL has been widely used as a model protein in research related to protein folding, unfolding, and aggregation as its structural information is well-defined. Moreover, it shares a high degree of sequence and structural homology with human lysozyme [10,11], which is affiliated with familial lysozyme systemic amyloidosis [12]. Numerous studies have demonstrated that HEWL is prone to fibrillate in a heated and acidic

* Corresponding author at: Protein Research Chair, Department of Biochemistry, College of Science, King Saud University, Saudi Arabia.
E-mail address: moskhan@ksu.edu.sa (M.S. Khan).

https://doi.org/10.1016/j.ijbiomac.2018.07.112
0141-8130/

environment [13], a concentrated ethanol solution [14], a concentrated solution of guanidine hydrochloride [15], and a vigorously agitated condition [16]. Therefore, HEWL serves as an excellent model system to study *in vitro* phenomena associated with fibril formation. Sodium dodecyl sulfate (SDS), an anionic surfactant having negatively charged the head group with a hydrophobic tail mimicking the structure of lipid molecules of biological membranes. SDS is a common denaturant that destroys protein's native conformation. It provides an anionic micellar interface that has been shown to accelerate the aggregation of Aβ (1–40) over a limited range (low SDS) of concentrations [17]. Since the conditions required to induce aggregation varies from protein to protein, the present study was designed carefully to induce protein aggregation or amyloid formation with SDS by choosing appropriate conditions based on its concentration.

Polyphenols and flavonoids have drawn considerable attention due to their potential role in neurodegenerative and cardiovascular diseases as well as for their anticarcinogenic, antioxidative, anti-inflammatory properties that have increased their application for medicinal and pharmaceutical purposes [18–21]. Rutin (quercetin-3-O-rutinoside) is one such flavonoid with a wide range of biological activities. It comprises quercetin and the disaccharide rutinose (rhamnose and glucose). Rutin is found in many plants (such as buckwheat seeds), fruits (such as citrus fruits), and vegetables [22,23]. Rutin is an important nutritional supplement because of its many pharmacological properties including anti-carcinogenic, cytoprotective, antiplatelet, antithrombic, vasoprotective, and cardioprotective activities [24,25]. Also, rutin is a powerful antioxidant and anti-inflammatory polyphenol [26]. Rutin and its analogs such as epigallocatechin-3-gallate (EGCG) and quercetin act as efficient free-radical inhibitors and are reported to rescue spatial memory impairment in rats with cerebral ischemia [27]. Pretreatment with rutin in chronic dexamethasone-administered mice attenuated cognitive deficits and brain impairment [28]. Numerous investigations demonstrate that the analogs of rutin can interfere with Aβ aggregation and neurotoxicity, prevent oxidative stress induced by Aβ, reduce Aβ42 levels in mutant human amyloid precursor protein (APP)-overexpressing cells, and decrease senile plaques in the brain of APP transgenic mice [29]. These effects of rutin analogs suggest that they are promising agents for the treatment of amyloidosis. The present study analyzes how rutin interferes with SDS mediated lysozyme fibrillation as well as with the pathogenic factors of protein aggregation.

2. Materials and methods

2.1. Materials

Hen egg white lysozyme (HEWL), Thioflavin T (ThT), 8-anilino-1-naphthalenesulfonic acid (ANS), rutin were purchased from Sigma Chemical Co. (St. Louis, USA). Buffer components (Tris-HCl) and SDS were obtained from SRL (India). PD-10 desalting column (GE, healthcare). The protein concentration was determined spectrophotometrically. All other reagents were of analytical grade.

2.2. Methods

2.2.1. Preparation of protein and ligand

The stock solution of lysozyme was prepared using its molar extinction coefficient of $\varepsilon_M = 37{,}970\ M^{-1}\ cm^{-1}$ at 280 nm [30]. A stock solution of lysozyme (70 μM) was prepared in 20 mM Tris-HCl buffer, pH 9.0. Working concentration of lysozyme was 5 μM for all our studies. A stock of SDS (20 mM) was prepared in double distilled Milli-Q water. Protein and ligand were further filtered through 0.22-μm filter. SDS was used in between 0.2 and 1 mM concentration range which is far less than critical micellar concentration (CMC) in tris buffer (8 mM) [30].

2.2.2. Turbidity measurement

Turbidity assay was used as an indicator to suggest the formation of protein aggregates. The absorbance of the native and SDS-treated lysozyme was carried out at 350 nm on UV–vis spectrophotometer (Ultrospec-2100 Pro, Amersham Bioscience). The concentration of the lysozyme was 5 μM, and SDS was varied between 0.2 and 1.0 mM.

2.2.3. Rayleigh light scattering (RLS) measurement

RLS analysis of HEWL (5 μM) in absence and presence of SDS (0.2–1.0 mM) was performed on a Jasco (FP-750) fluorescence spectrophotometer at pH 9.0. The excitation wavelength was fixed at 350 nm, and the emission spectra were recorded between 300 and 400 nm.

2.2.4. Kinetics of SDS- induced aggregation

SDS-induced aggregation kinetics of lysozyme was done by RLS measurements on Jasco (FP-750) fluorescence spectrophotometer at room temperature. Lysozyme was treated with different concentration of SDS (0–1.0 mM). The emission was recorded at the 350 nm with respect to time after excitation at 350 nm. Also, their aggregation kinetics was measured in the presence of rutin (10–30 μg/ml). 5 μM lysozyme was used and kinetics was obtained at pH 9.0. The excitation and emission slit width were fixed 5′5′ nm.

2.2.5. Steady-state fluorescence measurement

SDS-induced conformational changes in lysozyme were investigated using tryptophan fluorescence. Conformational changes in lysozyme treated with SDS were monitored on spectroflurometer (Jasco FP-750). The excitation of protein samples was performed at 295 nm, and the emission spectra were recorded over a wavelength range of 300–400 nm.

2.2.6. Surface hydrophobicity measurements

ANS (8-Anilinonaphthalene-1-sulfonic acid) is used for monitoring conformational changes in proteins and is specifically binds to hydrophobic domains of proteins [31]. A stock solution of ANS (hydrophobic dye) was dissolved in double distilled water, filtered and further its concentration was determined at 350 nm using a molar extinction coefficient, $\varepsilon_M = 5000\ M^{-1}\ cm^{-1}$ [32]. SDS-treated lysozyme samples were incubated with a 50-fold molar excess of ANS for 30 min in the dark. The samples were excited at a wavelength of 380 nm, and emission spectra were recorded in the wavelength range of 400–600 nm. All spectra were corrected for their appropriate blanks.

2.2.7. CD measurement

Far-UV CD spectra were acquired using applied photophysics Chirascan spectrophotometer. Far-UV CD spectra of lysozyme treated with different concentration of SDS were recorded between 200 and 250 wavelength ranges. The protein concentration was 5 μM, and a quartz cuvette of 0.1 cm path length was used.

2.2.8. Thioflavin T (ThT) fluorescence

A stock solution of ThT was prepared in distilled water and filtered with 0.45 μM Millipore filter. A molar extinction coefficient ($\varepsilon_M = 36{,}000\ M^{-1}\ cm^{-1}$) was used to determine the concentration of ThT at 412 nm [33]. Aliquots (5 μM) of HEWL solutions, pre-incubated overnight with different concentrations of SDS in 0–1.0 mM range, were mixed with ThT (10 μM) followed by 30 min of incubation in the dark. Fluorescence spectra were measured on Jasco (FP-750) fluorescence spectrofluorometer at excitation and emission wavelengths of 440 and 450–550 nm, respectively. Spectra were appropriately corrected for their respective blanks.

2.2.9. Congo red (CR) binding

CR dye has been extensively used as an indicator of the presence of protein aggregates/fibrils. CR stock solution was prepared in Milli-Q water, and its concentration was calculated using molar extinction

coefficient of 45,000 M^{-1} cm^{-1} at 498 nm. HEWL (5 μM) with and without 0.2 mM SDS were incubated for 12 h. After centrifugation, aggregated and non-aggregated samples were further incubated with CR (5 μM) for 30 min in the dark. The absorbance spectra (400–600 nm) of the samples were recorded on a Carry 60UV–visible spectrophotometer in a 1 cm path length cuvette.

2.2.10. Aggregation kinetics of lysozyme in the presence of rutin: ThT fluorescence measurement

The amyloid inhibitory potential of rutin for SDS-mediated amyloidogenesis of HEWL was investigated using ThT fluorescence assay. SDS (0.2 mM)-mediated lysozyme fibrillation was treated with various concentrations of rutin ranging from (10–30 μg/ml) and measured for ThT binding. 5 μM protein sample was aliquoted after certain interval of time and treated with 20 μM ThT solution. The spectrum was obtained between 450 and 550 nm after excitation at 440 nm. ThT Fluorescence intensity at 482 nm against various time intervals was plotted. All data are fitted by using following equation:

$$F = F_i + m_i t + \frac{F_f + m_f t}{1 + e - [(t - to)/\tau]}$$

where F is the fluorescence intensity at time t, and t_0 is the time to attain 50% of maximal fluorescence intensity. (Fi + mit) and (Ff + mft) represent the initial base line related to the induction time and final constant line, respectively. The apparent rate constant for fibril growth is given by 1/τ, and the lag time is calculated by $t_0 - 2\tau$.

2.2.11. Cytotoxicity measurement via cell viability (MTT) assay

MTT (3, (4, 5-dimethylthiazol-2-yl) 2, 5-diphenyltetrazolium bromide) reduction assay was used to measure the cell viabilities of SH-SY5Y. MTT in the presence of viable cells get reduced to form blue formazan crystals; toxicity leads to inhibition of formazan production [34]. For the MTT reduction assays, SDS was removed from aggregated lysozyme using PD-10 desalting column (GE healthcare, USA). Further, aggregated lysozyme (3 μM) in the absence and presence of rutin (10–50 μg/ml) were added to SH-SY5Y cells in 96-well plates. Cells were seeded at 5000 cells/well on 96-well plates and incubated for 24 h before the treatment. MTT was added to the culture medium to yield a final concentration of 0.5 mg/ml and incubated for 4 h at 37 °C in the CO_2 incubator. The supernatant carefully removed, and DMSO (200 μl) was added and mixed. After incubation, absorbance at 585 nm was measured using a Micro-plate absorbance reader (Chameleon, USA).

2.2.12. Morphological analysis of lysozyme aggregates by TEM

The morphology of SDS-induced aggregates of the lysozyme was examined by transmission electron microscopy (TEM). JEOL transmission electron microscope operating at an accelerating voltage of 180 kV was used to capture the morphology of aggregates. 5 μl of aggregated samples in the absence and presence of rutin were applied on 200-mesh, copper grid covered by the carbon stabilized the formwar film. 1% uranyl acetate was used for negative staining. The concentrations of lysozyme were fixed 5 μM in all the samples. The images were viewed at high resolution.

2.2.13. In situ studies

2.2.13.1. Animal treatment. Six adult male Swiss albino mice (35–40 g, 2–3 months old) were purchased from the central animal house, Department of Pharmacy, King Saud University, Riyadh, KSA. They were housed and treated under the hygienic conditions (25 ± 5 °C with 12 h day: night cycle) as per the institutional guidelines. All the rodents were acclimatized for a week on a standard pellet diet and fresh drinking water *ad libitum*. They were sacrificed by cervical dislocation, and the blood was collected in vacuum collecting tubes (EDTA coated) and kept in the cold.

All the animal-based experiments were conducted by the guidelines for the care and use of experimental animals by the Committee for Control and Supervision of Experiments on Animals and the National Institutes of Health. The treatment method and study protocol (care and handling of experimental animals) were approved by the Animal Ethics Committee of the Zoology Department in the College of Science at King Saud University, Riyadh (KSA).

2.2.13.2. Isolation of lymphocytes. The isolation of the lymphocytes was done by the method by Chibber et al. (2011) [35]. Three milliliters of blood from each mouse was diluted in Ca^{2+} and Mg^{2+} free PBS separately. The separation of the lymphocytes from these samples was achieved by mild centrifugation using Histopaque 1077. The cells thus separated were finally mixed with RPMI-1640. All the six samples were appropriately labeled and stored in microfuge tubes (Eppendorf, Germany) in cold condition.

2.2.13.3. Viability assessment of lymphocytes. Viability of the lymphocytes was assessed before the start and after the end of the reaction using trypan blue exclusion test [36].

2.2.13.4. Treatment of lymphocytes. One ml of cells (~100,000) was pippetted in 4 separate microfuge tubes. The first tube was taken as control (Group I). 20 μl of aggregated protein and polyphenol rutin were added in second and third tubes denoted as group II and III respectively. Their incubation was allowed for 2 h at room temperature. 20 μl of the protein was added to the fourth tube (group IV); to which 10 μl of the polyphenol was added after 2 h of incubation that was further kept under incubation for 2 h.

2.2.13.5. Comet assay (single cell electrophoresis). Isolated lymphocytes were exposed to aggregates of HEWL in a total reaction volume of 1.0 ml of 20 mM phosphate buffer pH 7.2. Incubation was performed at 37 °C for 1 h. After incubation, the reaction mixture was centrifuged at 700 ×*g*, the supernatant was discarded, while the pellet containing lymphocytes were resuspended in 100 ml of PBS and processed further for Comet assay. Remaining all the steps of comet assay of aggregated protein was performed under alkaline conditions with standard protocol [37].

2.2.14. Molecular docking of rutin with lysozyme

Different modules of Schrödinger suite (Schrödinger, LLC, New York, NY, USA) were used to perform different steps involved in molecular docking. All the computational work was performed on Intel® Xenon® E3-1245v5 8C @ 3.50 GHz with 28.0 GB RAM and 1 TB hard disc running Windows 7 and equipped with NVIDIA Quadro M2000 graphics card.

2.2.14.1. Proteins/ligand retrieval and preparation. Maestro was used for all the steps involving protein and ligand preparation, receptor grid generation and docking. The X-ray crystal structure of ligand-bound lysozyme (PDB Id: 1HEW) at 1.92 Å resolution was retrieved from PDB database (http://www.rcsb.org/pdb). Before molecular docking, the structure of lysozyme was prepared using "protein preparation wizard" of GLIDE at pH 9.0 to simulate the experimental conditions. Missing loops and any side chains were added using PRIME. Protein was then optimized to create H-bond network, and finally, energy was minimized using an OPLS2005 force field. The structure of rutin was drawn using 2D sketcher of Schrodinger suite and optimized for docking by assigning the bond orders and angles using LigPrep module. 2D structure of rutin was converted into the 3D structure, and the energy was minimized using OPLS2005. The ionization state of rutin was generated at pH 7.0 ± 2.0 with the help of Epik module of LigPrep, keeping other parameters to default values.

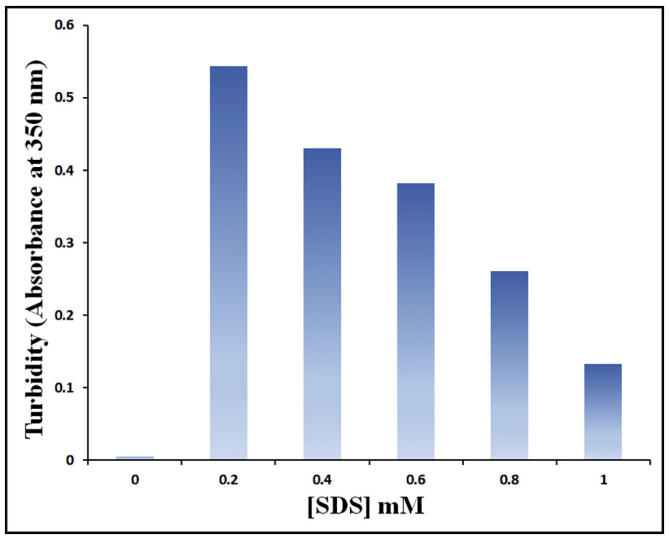

Fig. 1. Turbidity analysis of SDS-lysozyme solution. Turbidity measurements were carried out on samples to detect the quantity of aggregates at 350 nm. Lysozyme (5 μM) was incubated with and without different concentrations (0.0–1.0 mM) of SDS at pH 9.0. All the samples were incubated for 12 h before measurements at room temperature.

2.2.14.2. Grid generation and molecular docking. The active site of lysozyme was predicted by SiteMap. The binding site with the best site score was selected as the most probable active site of the protein. The grid box was generated by selecting the centroid of the predicted site as the centroid of the grid box. Molecular docking of rutin with lysozyme was performed using GLIDE in four different stages namely high throughput virtual screening (HTVS), standard precision (SP), extra precision (XP) and induced-fit docking (IFD). Post-docking analysis and visualization were performed on Maestro.

2.2.14.3. Molecular Mechanics-General Born Surface Area (MM-GBSA) calculations. The effect of solvent on the binding property of rutin with lysozyme was also elucidated by performing Molecular Mechanics-General Born Surface Area (MM-GBSA) using molecular mechanics (MM) force fields and implicit solvation solvent model, which incorporates the OPLS 3 force field, VSGB solvent model, and rotamer search algorithms [19]. In this study, we have used Prime module of Schrodinger suite (Prime, Schrödinger, LLC, NY, USA) for calculating MM-GBSA according to the following equation:

$$\Delta G = \text{E\_complex (minimized)} - [\text{E\_ligand (minimized)} + \text{E\_receptor (minimized)}]$$

MM-GBSA was calculated keeping the default setting. The protein-ligand complexes were ranked based on their binding free energy calculation.

2.2.15. Statistical analysis

All the experiments were conducted in triplicates. All the experimental data were represented as Mean ± SEM analyzed by GraphPad Prism 5 software. The data were analyzed by one-way ANOVA with Tukey's post-hoc and p-value was selected <0.05 as statistically significant calculated by the software. The number of asterisk mark* and #indicates the extent of statistically different from the respective positive control (group I) and Control positive (group II) values respectively *in situ* studies.

3. Result and discussion

HEWL is one of the best known globular proteins for which three-dimensional structure, folding-unfolding mechanism, and conformational stability have been extensively studied [38,39]. Many studies have exploited lysozyme to elucidate the nature of amyloid fibrillization with the aim to understand various aspects of amyloid formation in humans [40,41]. Moreover, HEWL is highly homologous in the sequence

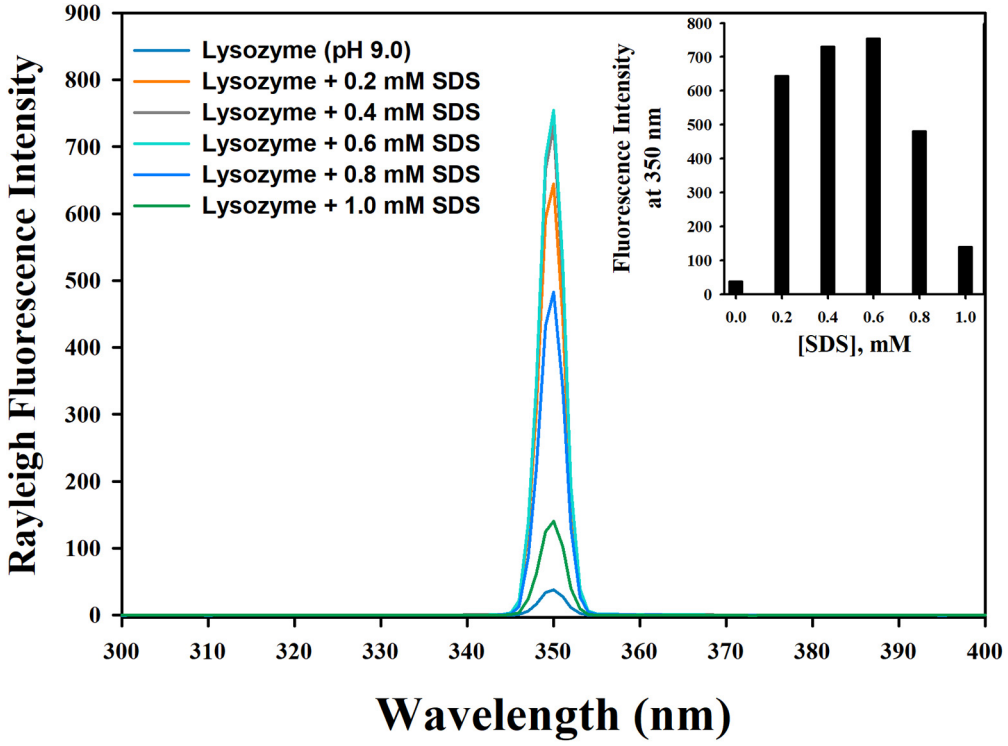

Fig. 2. Rayleigh scattering measurement. Lysozyme (5 μM) was exposed to different concentrations of negatively charged surfactant (SDS) from 0.0 to 1.0 mM at 20 mM tris-glycine buffer pH 9.0 and their fluorescence emission spectra was recorded between 300 and 350 nm after excitation at 350 nm. (Inset) shows the fluorescence intensity at 350 nm under the same conditions.

and structure to human lysozyme. Human lysozyme is known to form massive amyloid deposits in liver and kidneys of the patients suffering from fatal hereditary non-neuropathic systemic lysozyme amyloidosis. Human lysozyme variants namely Ile56Thr and Asp67His are the most amyloidogenic and their deposits often lead to massive hemorrhaging resulting in the death of the patient [42]. *In vitro*, HEW or human lysozymes form amyloid aggregates at conditions which lead to the transformation of native molecules into partially unfolded states (low pH, high temperature and presence of denaturants, salts and others). The partially unfolded state allows intermolecular interactions of the amyloidogenic regions leading to the formation of amyloid fibrils. Studies indicate that highly amyloidogenic regions consist of residues from 57 to 107 or from 49 to 101 [43,44]. A convenient strategy for induction of aggregation in such system requires neutralization of positive charge along with increased hydrophobic interactions. Both of these requirements can be fully fetched by an amphipathic anionic detergent such as SDS. SDS contains negatively charged polar head groups and a twelve carbon long non-polar hydrophobic tail. In general, the negatively charged head group of SDS interacts with positive charge developed on protein and the hydrophobic region makes contact with its protein counterpart by repelling the water molecules wrapped around the protein molecule. As a result, solute-solvent interactions are perturbed leading to the induction of aggregates [45]. Aggregation occurred readily in enzymes possibly due to the provision of favorable hydrophobic interaction by SDS, thus collapsing the molecules into aggregates. Polyphenols are naturally occurring compounds which have been reported to be proficient amyloid inhibitors. They have also been found to possess the potency to disaggregate preformed fibrils [46]. We have investigated the effect of rutin, a polyphenol on HEWL fibrillation induced by an anionic surfactant (SDS). HEWL fibrillation was carried out by incubating the protein with various concentration of SDS for 12 h at room temperature. Results show that lysozyme undergoes amyloidogenesis most efficiently at 0.2 mM SDS, and rutin is capable of inhibiting HEWL fibrillation in a dose-dependent manner. SDS mediated aggregation process of HEWL, as well as the inhibitory efficacy of the rutin, was monitored using multi-spectroscopic and microscopic techniques.

3.1. Turbidimetric aggregation analysis

The self-association process of SDS treated HEWL was investigated using solution turbidity assay by recording absorbance at 350 nm. An increase in the absorbance value at 350 nm indicates greater aggregation due to an increase in the scattering of light by aggregated particles. Fig. 1 shows that in the absence of SDS, the absorbance value is almost negligible indicating no aggregation for control HEWL. The turbidity increased remarkably upon addition of SDS, showing maximum value at 0.2 mM SDS with around 109-fold increase relative to the native HEWL. The results clearly suggested the formation HEWL aggregates in the presence of 0.2 mM SDS. Upon further sequential additions of SDS from 0.4 mM to 1.0 mM, the turbidity showed a decline as compared to HEWL incubated with 0.2 mM SDS. However, the turbidity was still on the higher side as compared to native HEWL. The possible explanation for this could be at lower concentration of SDS (0.2–0.6 mM) ionic interactions was dominant between HEWL and SDS leading to conformational changes and formation of aggregates. Lower concentration of SDS induced aggregates has been reported for many proteins [30]. As evident in Fig. 1, higher concentration of SDS (0.8–1.0 mM) less turbidity was observed, suggesting stabilizing or solubilizing effect. This could be due to hydrophobic or crowding affect as CMC of SDS in tris buffer is 3.4 mM [47].

3.2. RLS measurements

In addition to measuring absorbance at 350 nm, measuring the scattering of light by recording fluorescence intensity at 350 nm proves to be a valid indicator for the formation of protein aggregates. As is evident from Fig. 2, there was an almost twenty-fold increase in light scattering when HEWL was incubated with 0.2–0.6 mM SDS, suggesting the formation of aggregates. However, the scattering of light was reduced on further increasing surfactant concentration above 0.8 mM. Moreover, at 1.0 mM SDS concentration, scattering of lysozyme was only 3.7-fold higher than the native state of the protein. The possible reason could be the fact that above 0.6 mM SDS concentration range, the secondary structure of lysozyme was getting stabilized rather than unfolded.

3.3. Kinetics of SDS-induced aggregation

Kinetics of lysozyme aggregation in the presence of SDS is shown in Fig. 3. From the figure, it was observed that the fluorescence intensity at 350 nm is significantly less in the absence of SDS, suggesting that lysozyme alone do not form aggregates. However, in the presence of 0.2 mM SDS, maximum increase in the fluorescence intensity was recorded just after mixing, demonstrating SDS induced aggregation of lysozyme does not contain lag phase. The absence of lag phase suggesting that SDS-induced aggregation of lysozyme is nucleus independent. With further increase in SDS concentration, RLS at 350 decreased, illustrating stabilization of lysozyme. Rutin inhibited the aggregation of lysozyme as indicated by decrease in intensity at 350 nm (Fig. 3b).

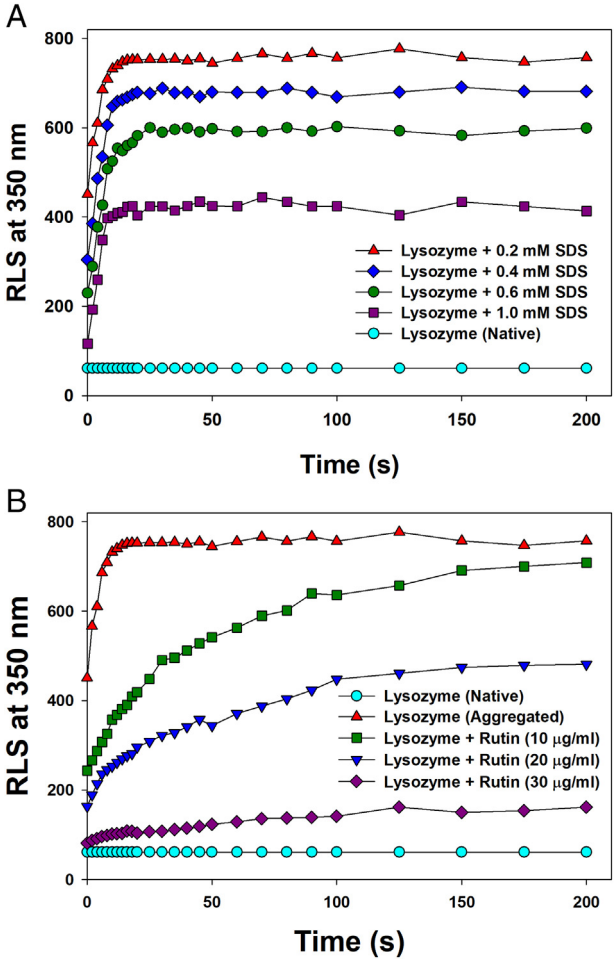

Fig. 3. Kinetics of SDS-lysozyme interactions. SDS-induced aggregation kinetics of lysozyme was done by RLS measurements. 5 μM lysozyme was treated with different concentration of SDS (0–1.0 mM). The emission was recorded at the 350 nm with respect to time after excitation at 350 nm. RLS kinetics was also measured in the presence of 0–30 μg/ml rutin.

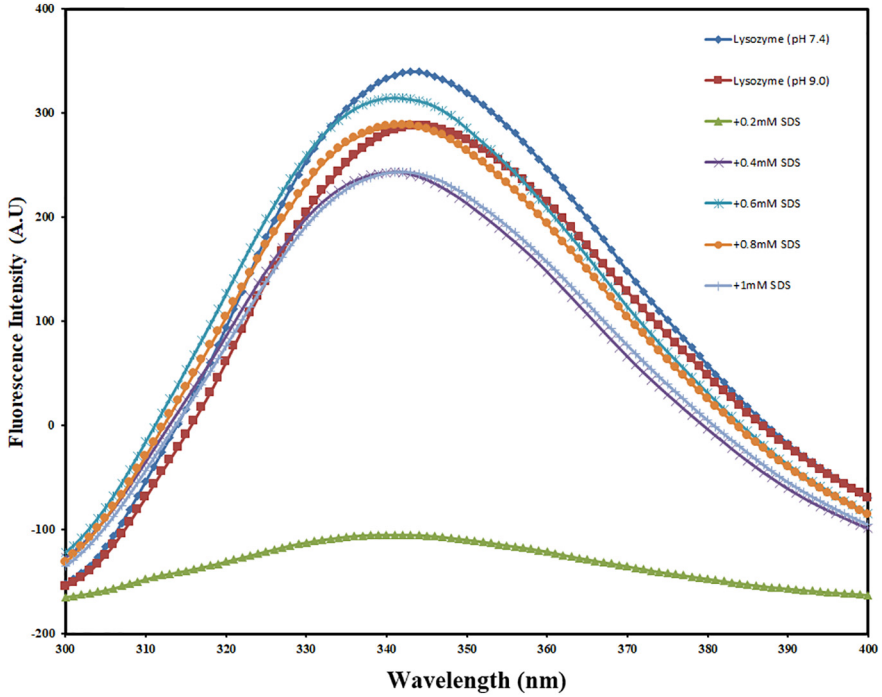

Fig. 4. Intrinsic fluorescence analysis. Tryptophan fluorescence of SDS-lysozyme solution was monitored using excitation wavelength of 295 nm and emission were recorded in 300–400 nm range. Lysozyme was used in the concentration of 5 μM in the absence and presence of 0.0–1 mM SDS. (For interpretation of the references to color in this figure, the reader is referred to the web version of this article.)

3.4. Steady-state fluorescence measurements

Intrinsic fluorescence is a very sensitive and specific tool to determine and investigate the conformational changes in a protein during experimental studies. Intrinsic fluorescence spectra of HEWL samples incubated in the presence of different SDS concentrations are shown in Fig. 4. The intrinsic fluorescence of lysozyme was drastically quenched in the presence of 0.2 mM SDS, suggesting major conformational changes in the protein and loss of their tertiary structure. With further increase in SDS concentration (0.4–0.6 mM), a blue shift of 3 nm was observed, which indicated a gross structural derangement of HEWL molecules, possibly due to aggregation. Further, the

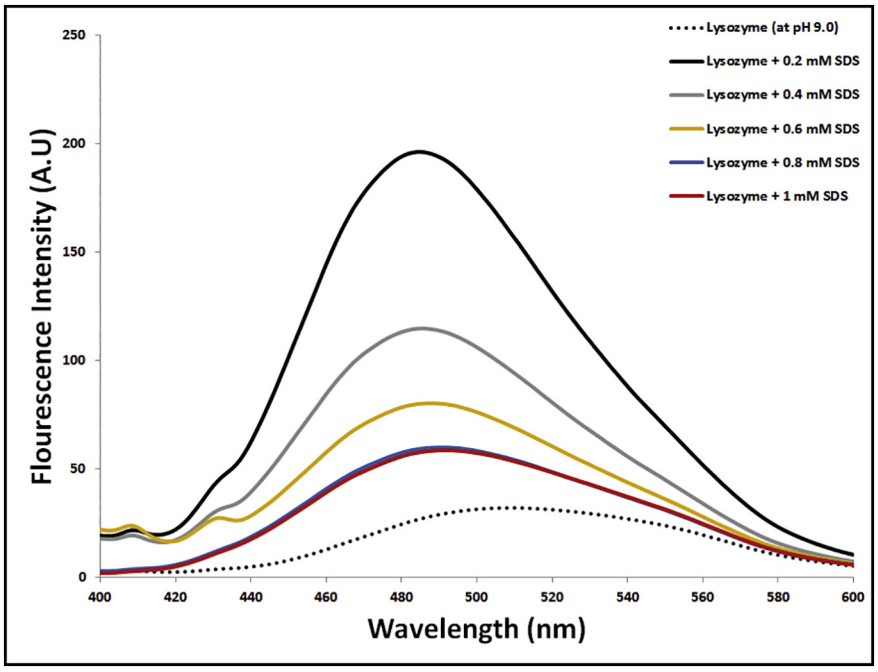

Fig. 5. Surface hydrophobicity of lysozyme in the presence of SDS. SDS-lysozyme solution after overnight incubation was analyzed for its hydrophobicity. 250 μM ANS (8-Anilino-1-naphthalenesulfonic acid) dye was added and incubated further for 30 min. Spectrum were obtained between 400 and 600 nm, after excitation at 380 nm. (For interpretation of the references to color in this figure, the reader is referred to the web version of this article.)

Table 1
Secondary structure content of SDS-treated lysozyme.

	Reported value (%)	Experimental (%)						
	CDSSTR	pH 7.4	pH 9	0.2 mM SDS	0.4 mM SDS	0.6 mM SDS	0.8 mM SDS	1.0 mM SDS
Alpha helix	44	43	53	19	39	58	62	60
Beta sheet	10	11	12	26	14	11	16	13
Random coil	46	26	21	30	28	19	15	17
Turns	–	20	14	25	20	13	8	11

fluorescence intensity and wavelength maxima of lysozyme in the presence of higher SDS concentration (0.8–1.0 mM) regained a value which was similar to that of protein in the native state. The results indicate that SDS in the concentration range of 0.8–1.0 mM had a stabilizing or solubilizing effect on lysozyme. Moreover, the fluorescence intensity and wavelength maxima of native HEWL at pH 7.4 were found to be 339.606 and 343 nm respectively. Similarly, the fluorescence intensity and wavelength maxima of native HEWL at pH 9.0 were found to be 287.653 and 344 nm respectively. The decrease in fluorescence intensity along with a red-shift of 1 nm indicated that the conformation of lysozyme was slightly altered at pH 9.0 as compared to that at pH 7.4.

3.5. Surface hydrophobicity measurements

To investigate the relative exposure of hydrophobic regions and to characterize the intermediate states involved in the passage from the folded to the unfolded state or *vice versa* during anionic detergent induced fibrillation of HEWL, ANS binding studies were performed (Fig. 5). We found that there was no significant binding of ANS to native HEWL in the absence of SDS (red dotted curve) due to the fact that the hydrophobic site groups are hidden inside the native HEWL with folded and compact structure. Whereas HEWL incubated with 0.2 mM SDS showed a prominent increase of around 6-fold in intensity with a significant blue shift from 510 to 486 nm. We also observed same blue shift (~24 nm) although with comparatively low intensities in the ANS fluorescence for HEWL incubated with 0.4–0.6 mM SDS. The results indicated that at lower concentration of SDS (0.2–0.6 mM), HEWL was likely in partially folded conformation with abundant exposed hydrophobic surfaces. HEWL samples at higher doses of anionic surfactant (0.8–1.0 mM) showed only about 1.8-fold hike in ANS intensity and a blue shift of 19 nm thereby indicating less exposure of hydrophobic patches as the protein is apparently stabilized in this range of surfactant.

3.6. Secondary structure analysis: far UV-CD

The circular dichroism spectroscopy (CD) was utilized to investigate the changes in the secondary structure of lysozyme associated with its fibrillization in the presence of different concentrations of SDS relative to the native control (Table 1, Fig. 6). CD spectrum of native lysozyme indicates a high content of the α-helical structure as reflected by pronounced ellipticity signals at 208 and 222 nm (Fig. 6, blue curve). At 0.2 mM SDS, the protein lost most of its secondary structure as indicated by loss in negative ellipticity along the whole spectrum. This CD spectrum indicates HEWL transformation into amyloid fibrils with high content of β-structure as indicated by retention of some negative ellipticity at ~218 nm (Fig. 6, dark red curve). The CD spectra recorded in presence of increasing concentration of anionic detergent are also presented in Fig. 6. At low SDS concentrations (0.4 and 0.6 mM) the spectra are similar to the spectrum detected for lysozyme fibrils at 0.2 mM SDS as sharp decrease in negative ellipticity signal around 208/222 nm while as retention in negative maximum at ~218 nm is observed (Fig. 6 green and purple curves). At higher SDS concentrations (0.8 and 1.0 mM) the spectra exhibit a steep change characterizing the high content of α-helical secondary structure resembling to that of the native lysozyme

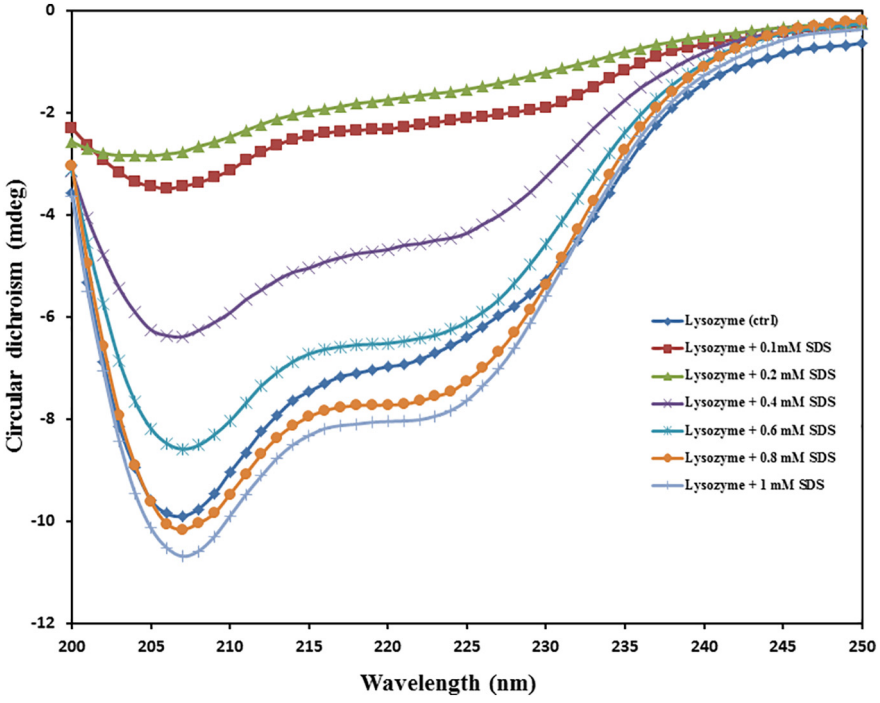

Fig. 6. Secondary structural conformational analysis. Far-UV CD spectra of lysozyme (5 μM) in the absence and presence of SDS (0–1.0 mM). (For interpretation of the references to color in this figure, the reader is referred to the web version of this article.)

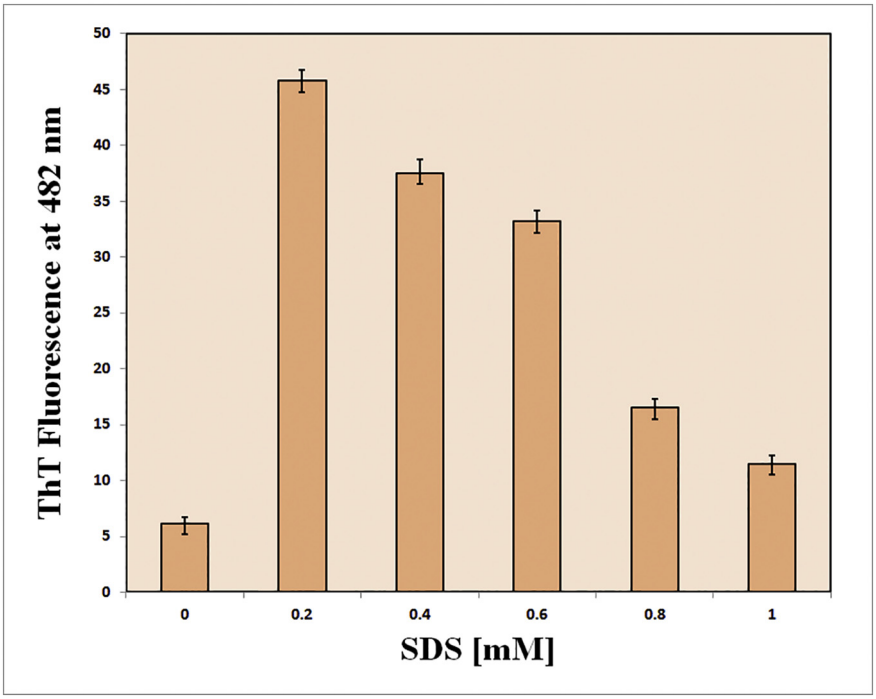

Fig. 7. Amyloid formation: ThT fluorescence spectra of lysozyme incubated at 25 °C for 12 h in absence and presence of SDS (0–1.0 mM).

(Fig. 6 black and red curves). Thus at concentrations higher than 0.6 mM of SDS, the shape of the CD spectra are similar to the CD spectrum of the native lysozyme possibly due to the stabilizing effects of the anionic detergent/surfactant on lysozyme. It can be safely concluded that SDS at lower concentrations of up to 0.4 mM causes unfolding of the HEWL which consequently leads to the aggregation and amyloidogenesis of the enzyme, while higher concentrations stabilize its secondary structure. The findings also show that 0.2 mM concentration of SDS was the most significant in bringing about aggregation of the HEWL. To further support secondary structural changes in lysozyme under SDS treatment, FTIR spectroscopy was measured. The observed results clearly showed lysozyme incubated with 0.2 mM SDS, undergoes conformational changes from alpha helix to β-sheet as peak shifted from 1656 to 1633. With further increase in SDS concentration various secondary structures dominated by β-sheet and β-turn are formed (Supplementary Fig. 1).

3.7. Amyloid analysis: thioflavin T assay

Thioflavin T is an important and sensitive assay for the identification of protein aggregates and fibrils *in vitro*. ThT dye shows enhanced fluorescence upon binding to intermolecular β-sheets present in protein aggregates but not with native and soluble protein [48]. In the present study, ThT fluorescence assay was performed to complement light scattering and turbidometric results about the presence of HEWL aggregates induced by SDS. As depicted in Fig. 7, ThT fluorescence signal of native HEWL was very weak, indicating negligible binding of ThT to native HEWL. At 0.2 mM SDS, there was a marked increase in the intensity of

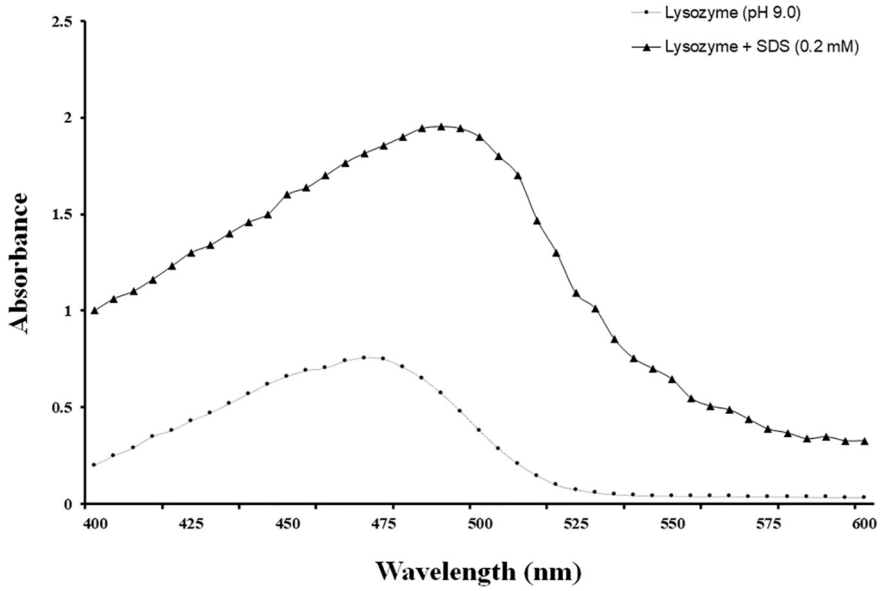

Fig. 8. Congo red binding: Amyloid fibril formation in lysozyme in the presence of SDS (0.2 mM) was measured by Congo red binding.

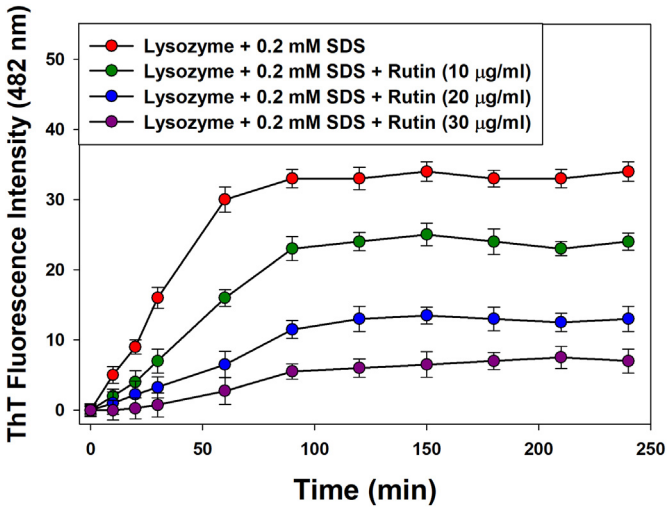

Fig. 9. Aggregation kinetics of lysozyme in the presence of rutin: ThT fluorescence kinetics of lysozyme (5 μM) amyloid aggregation with respect to incubation time (0–250 min) in absence and presence of 10–30 μg/ml rutin. Results have been represented as Mean ± SEM (n = 3).

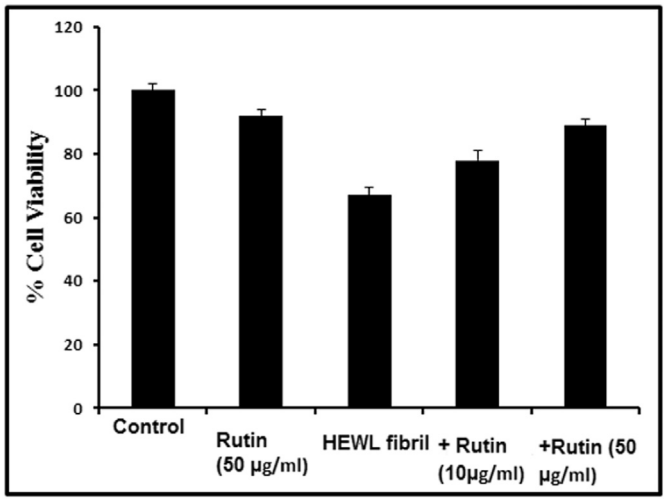

Fig. 10. Cytotoxicity of fibrillated lysozyme and their attenuation by rutin. MTT reduction assay for cell cytotoxicity of 0.2 mM SDS treated lysozyme fibrils in absence and presence of rutin (10 and 50 μg/ml) on SH-SY5Y cell lines. Control represents the cells without exposed to lysozyme fibrils.

ThT fluorescence (about 88%), indicating the presence and formation of abundant HEWL fibrillar aggregates. A similar trend was also observed at 0.4 mM and 0.6 mM SDS concentrations, accounting for an increase of about 86% ThT signal relative to the native lysozyme. At further higher concentrations of SDS from 0.8 mM to 1.0 mM, the respective ThT signals were lowered relative to lower concentrations but still higher than that of native HEWL. The most convincing reason behind this could be due to the stabilizing effects of anionic detergent at higher doses. These findings further indicate and validate that the most effective SDS concentration for inducing fibrillar aggregates in HEWL was 0.2 mM.

3.8. Congo red binding

Congo red assay is utilized to probe for the presence of β-sheet structure associated with ordered protein aggregates. An enhanced absorbance and red-shifted spectral maximum indicate the presence of increased cross β-sheet rich structures which is a prime feature of protein aggregates [49]. In support the findings of ThT assay, Congo red binding assay was also performed to detect amyloid formation of HEWL. Congo red binding absorption spectra of HEWL in the absence and presence of SDS are shown in Fig. 8. As shown in the figure, HEWL sample incubated with 0.2 mM SDS had significantly bound Congo red and shifted the spectral properties of Congo red relative to the native HEWL. An increase in Congo red absorbance supplemented with a red shift of the spectral maximum indicated the formation of amyloid fibrils. This is a typical feature of amyloid fibrils and has been observed in earlier reports also [49].

3.9. Aggregation kinetics of lysozyme: rutin as anti-amyloidogenic polyphenol

ThT is an extrinsic fluorophore that exhibits fluorescence upon binding with characteristic cross β- sheet structure. Here, we have used ThT dye to monitor the aggregation kinetics of SDS-mediated lysozyme and their suppression in the presence of polyphenols rutin with respect to ThT fluorescence intensity. Fig. 9 shows the aggregation kinetics of lysozyme with respect to incubation time. The ThT fluorescence intensity starts increasing just after mixing of lysozyme with 0.2 mM SDS, suggesting lack of lag phase and nucleation independent aggregation. However, In the presence of rutin, ThT fluorescence intensity decreased and their lag phase was found to be increased to 18.21 min in the presence of 30 μg/ml rutin (Table 2). This delay in lag time also slows down the apparent growth rate of amyloid formation. Polyphenols have been reported to inhibit aggregation and amyloid formation of many proteins [50–55]. This could be due interaction of aromatic rings to hydrophobic groups or ROS scavenging activity of polyphenols like rutin [50].

3.10. Cytotoxicity and their attenuation by rutin: MTT assay

The cytotoxicity associated with SDS-induced HEWL aggregates and the potential cytoprotective role of rutin against this amyloid toxicity in the human neuronal cell line (SH- SY5Y) was determined using MTT assay. As shown in Fig. 10, cell viability was decreased to 67% in the presence of HEWL aggregates, suggesting the neuronal apoptosis by these HEWL aggregates. Moreover, rutin had a dose-dependent effect on cell viability which increased from 67% to 79% and 89% in the presence of 10 and 30 μg/ml rutin, respectively (Fig. 10). A higher concentration of rutin (50 μg/ml) had significantly attenuated cell toxicity by

Table 2
Kinetics of SDS-treated lysozyme in the presence of rutin.

Samples	Lag time, $t_o - 2\tau$ (min)	Apparent rate, $1/\tau$ (min^{-1})	RelativeThT fluorescence intensity (%)	% reduction in ThT fluorescence intensity
Lysozyme + 0.2 mM SDS	0.08	0.0698	100.0	–
Lysozyme + 0.2 mM SDS + 10 μg/ml rutin	5.25	0.0533	70.6	29.4
Lysozyme + 0.2 mM SDS + 20 μg/ml rutin	12.93	0.0480	38.2	61.8
Lysozyme + 0.2 mM SDS + 30 μg/ml rutin	18.21	0.0432	20.6	79.4

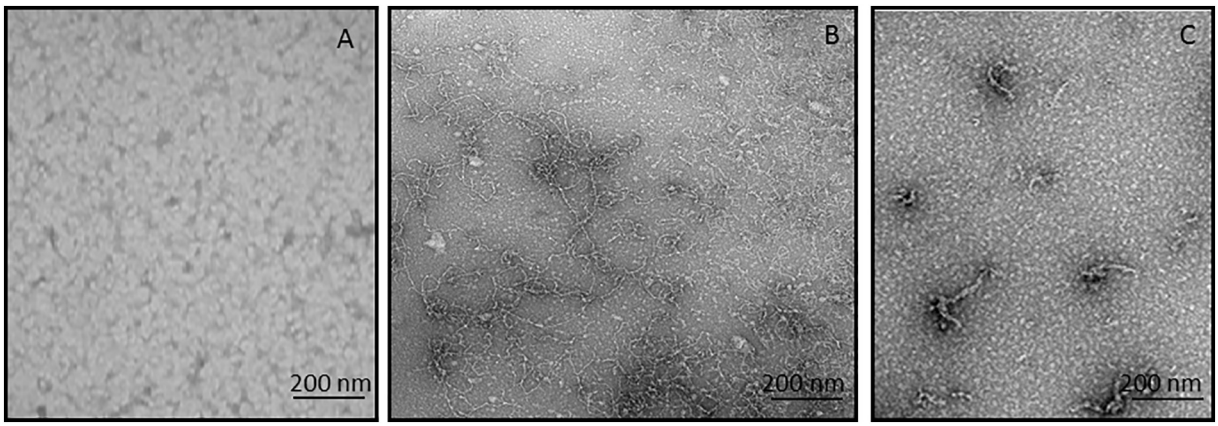

Fig. 11. TEM analysis: A drop of 5 μM lysozyme solution was placed on a grid followed by 1% uranyl acetate negative staining. (A) lysozyme solution at pH 9.0, (B) lysozyme treated with 0.2 mM SDS (C) SDS-treated lysozyme in the presence of 50 μg/ml rutin.

around 27% due to the inhibition of SDS-induced HEWL amyloid fibril formation process by rutin. Thus, the results are suggestive of the fact that the regained cell viability was due to the anti-amyloidogenic behavior of flavonoid (rutin) and its ability to inhibit cross-β-sheet conformation. Amyloid induced cytotoxicity and their attenuation by flavonoid have been reported earlier [41].

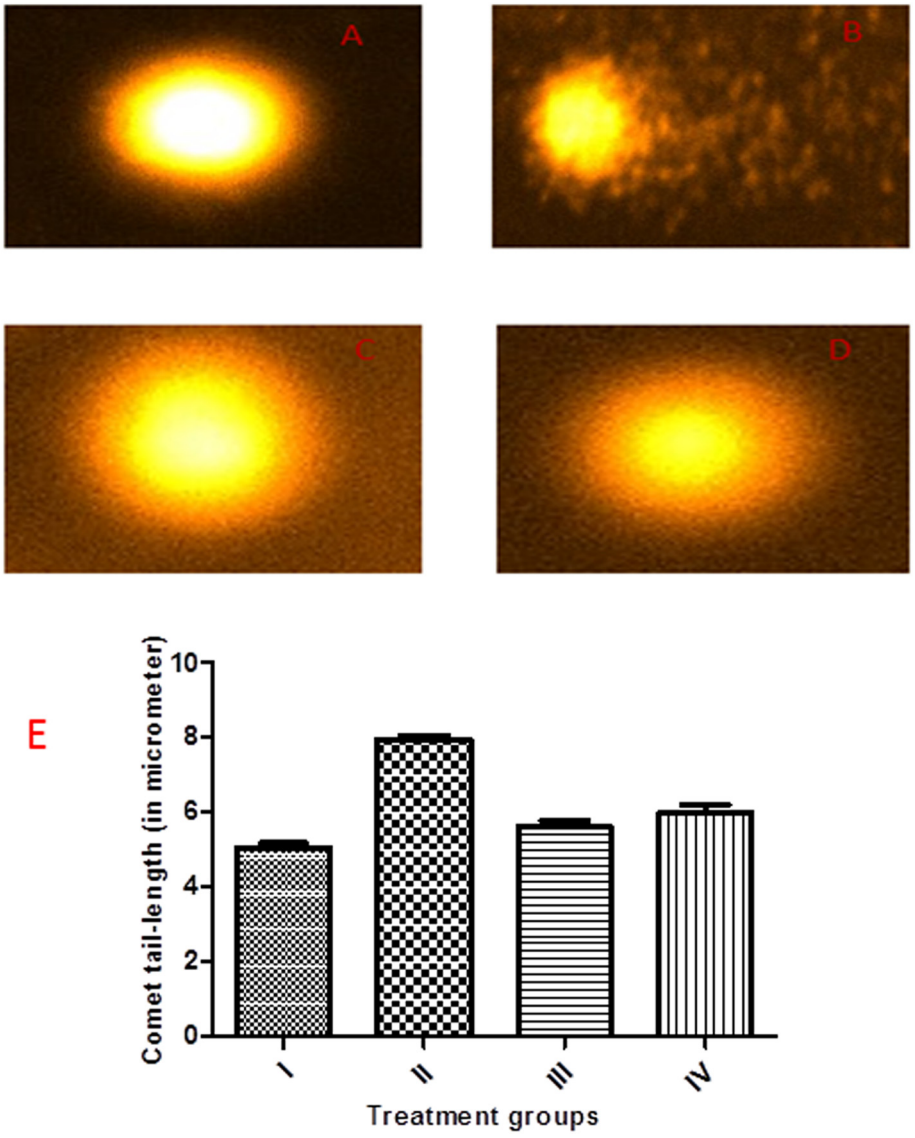

Fig. 12. Genotoxicity of aggregated lysozyme: Comet assay. Images of treated lymphocyte nuclei (A) lysozyme control in 20 mM phosphate buffer, pH 9.0 (B) lysozyme + SDS (0.2 mM) (C) lysozyme fibril + rutin (10 μg/ml) (D) lysozyme fibril + rutin (50 μg/ml).

3.11. Microscopic analysis (TEM)

The physical evidence of SDS-induced HEWL aggregation and the effect of polyphenol rutin on aggregation were analyzed with the help of transmission electron microscopy (TEM). As shown in Fig. 11, HEWL samples showed no aggregation whether amorphous or fibrillar (panel a), while as HEWL incubate with SDS (0.2 mM) without polyphenol displayed large, branched fibrils that are characteristic feature of amyloids (panel b). However, samples coincubated with rutin showed sparsely populated aggregates (panel c). These results demonstrate that rutin inhibits amyloid formation process in HEWL. The aggregation inhibition by rutin may be due to constraining the protein in its native state or the aggregation pathway might be somehow altered by rutin since significant changes in the morphology were observed. The results from TEM analysis are in clearly agreement with the ThT assay and demonstrate that rutin inhibits SDS induced HEWL amyloid formation.

3.12. Genotoxicity assessment: comet assay

To assess the genotoxic nature of SDS-induced HEWL aggregates and to support cytotoxicity results discussed above, we performed comet assay test. This test detects nicks with high sensitivity in damaged single- or double-strands of the nuclear DNA even if it is very less. In this assay, lymphocytes were treated with HEWL aggregates induced by 0.2 mM SDS (Fig. 12). In control (native HEWL), there was no genotoxic effect on lymphocytes in the presence of 20 mM phosphate buffer of pH 9.0 (Fig. 12A). However, when treated with SDS-induced HEWL aggregates (HEWL + 0.2 M SDS), lymphocytes showed DNA damage by 57.50% as compared to the control, group I (Fig. 12B). Moreover, we have also evaluated the effect of rutin in diminishing the genotoxicity of SDS-induced HEWL aggregates. We found that SDS-induced HEWL aggregates in the presence of 10 μg/ml rutin had significantly attenuated lymphocyte damage by 29.61% (Fig. 12C), while at higher rutin concentration (50 μg/ml), the damage was nearly prevented (Fig. 12D). The tail length of nuclei is represented in Fig. 12E. These results suggest that aggregated HEWL (0.2 M SDS + HEWL) has a predominant genotoxic effect on lymphocytes in relative to the native control *in vitro*. It also suggests that rutin exerts a concentration dependent preventive effect on HEWL aggregate mediated genotoxicity of lymphocytes. These findings are in good agreement with the above discussed MTT assay results which advocate that the attenuation in the genotoxicity of SDS-incubated HEWL aggregates was actually due to the aggregation inhibition potency of rutin.

3.13. Molecular docking studies

Molecular docking technique is a useful tool to elucidate the mechanism of binding of a ligand with protein [31]. In this study, the protein structure was first optimized to predict the charge on various ionizable amino acid groups of lysozyme at pH 9.0. The structure was then subjected to molecular dynamics to elucidate the energy minimized conformation of the enzyme at pH 9.0 (Supplementary Fig. 2). It appears from the Supplementary Fig. 1 that the structure of lysozyme at pH 9.0 was stabilized after 10 ns. We extracted the lysozyme structure at 10 ns for further studies. Different stereoisomers and charge on rutin was predicted at pH 9.0 using LigPrep wizard of Schrodinger suite. A total of 90 stereoisomers of rutin were predicted by Ligprep. Molecular docking of rutin with lysozyme was performed in four stages namely high throughput virtual screening (HTVS), standard precision (SP) docking, extra precision (XP) docking and induced-fit docking (IFD). HTVS was performed on 90 stereoisomers of rutin. The stereoisomers of rutin having more than −4.0 kcal/mol of binding energy (total 12 stereoisomers in number) were selected and subjected to SP docking (Supplementary Table 1). Out of the 12 stereoisomers of rutin, 9 showed a binding

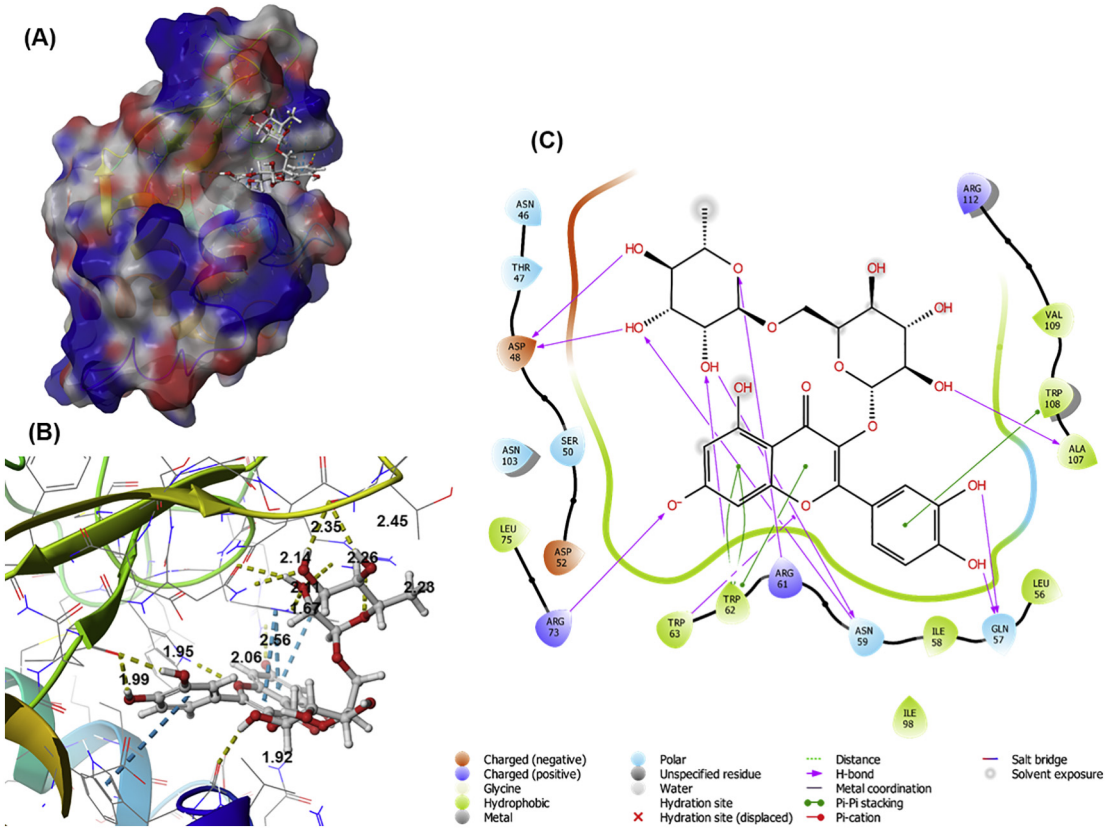

Fig. 13. Molecular docking of rutin with lysozyme. (A) Binding of rutin at the active site of lysozyme, (B) 3D representation of the interaction between rutin and lysozyme. The hydrogen bonds are displayed as yellow dash and their distances are mentioned in Å, (C) 2D representation of the involvement of various amino acid residues of lysozyme and molecular forces in stabilizing complex with rutin. (For interpretation of the references to color in this figure legend, the reader is referred to the web version of this article.)

Table 3
Molecular interactions and forces involved in forming lysozyme-rutin complex.

	Hydrogen bonds	Hydrophobic interactions	Binding energy (kcal/mol)	Binding affinity (M^{-1})	MM-GBSA (kcal/mol)
Lysozyme	Asp48[a], Gln57[a], Trp63, Asn103, Ala107, Arg112	Ile58, Trp62, Trp63, Ile98, Ala107, Trp108, Val109	−8.359	1.35×10^6	−16.479

[a] These residues form two hydrogen bonds.

affinity greater than −5.0 kcal/mol. These 9 rutin stereoisomers were then subjected to XP docking. The results showed that 5 stereoisomers of rutin interacted with lysozyme with an overall binding energy of more than −8.0 kcal/mol. The analysis of XP docking results indicated that amino acid residues in different loops and helices were involved in stabilizing the rutin-lysozyme complex. Hence, these 5 stereoisomers of rutin were subjected to induced fit docking (IFD) with lysozyme so as to accurately predict the involvement of different amino acid residues of lysozyme in interacting with rutin. Out of 5 stereoisomers, 3 showed a binding energy of greater than −13 kcal/mol.

The docking complex of rutin with lysozyme and the corresponding interacting amino acid residues are shown in Fig. 13(A, B & C). It is evident that rutin was bound at the active site of lysozyme and the interaction was stabilized by 11 hydrogen bonds and 9 hydrophobic interactions (Fig. 13 and Table 3). Other polar and charged residues such as Asp46, Thr47, Ser50, Asp52, Asn103 and Arg112 were also involved in the interactions. Rutin formed two hydrogen bonds each with Asp48, Gln57, and Asn59 amino acid residues of lysozyme. Moreover, Arg61, Trp62, Trp63, Arg73 and Asp107 of lysozyme were also found to form hydrogen bonds with rutin. The induced-fit docking score of lysozyme-rutin interaction was estimated to be −13.879 kcal/mol which corresponded to the binding affinity of $1.51 \times 10^{10}\ M^{-1}$. Subsequently, the effect of solvation on the rutin-lysozyme interaction was predicted by deducing MM-GBSA score. The MM/GBSA energy of lysozyme-rutin interaction was found to be −102.6425 kcal/mol. The magnitude of binding energy and the binding affinity indicates that rutin formed a very strong complex with lysozyme. The details ligand-protein interactions are presented in Fig. 13 and Table 3.

Recent computational as well as experimental aggregation profiling of HEWL have shown that there are three main "hot spots" located spanning the amino acid residues 24–34, 50–62 and 76–98 [56]. The amino acid residues corresponding to these "hot spot" are Ser24, Leu25, Gly26, Asn27, Trp28, Val29, Cys30, Ala31, Ala32, Lys33, Phe34, Ser50, The51, Asp52, Tyr53, Gly54, Ile55, Leu56, Gln57, Ile58, Asn59, Ser60, Arg61, Trp62, Cys76, Asn77, Ile78, Pro79, Cys80, Ser81, Ala82, Leu83, Leu84, Ser85, Ser86, Asp87, Ile88, Thr89, Ala90, Ser91, Val92, Asn93, Cys94, Ala95, Lys96, Lys97 and Ile98. The results of induced-fit docking of rutin with lysozyme indicated that rutin interacted with many key residues (Asp48, Ser50, Asp52, Leu56, Gln57, Ile58, Asn59, Arg61, Trp62 and Ile98) of the aggregation "hot spot" region of HEWL. Thus, it is clearly evident that rutin inhibits the aggregation propensity of HEWL by interacting strongly with the amino acid residues that are critically involved in the process of aggregation.

4. Conclusion

We have discussed here for the first time the effective and favorable approach to induce aggregation in proteins and explore the mechanism behind aggregation by anionic surfactants. The inhibitory potential of a flavonoid (rutin) against detergent induced aggregation of HEWL is also simultaneously depicted and established in this study. The study clearly comprehends that rutin exerts concentration dependent effect in preventing the fibrillation process of HEWL. The ThT binding assay indicates maximum inhibition of aggregation in the presence of 50 μg/ml rutin. Intrinsic and extrinsic fluorescence results suggest the involvement of gross structural changes in the presence of SDS which is more

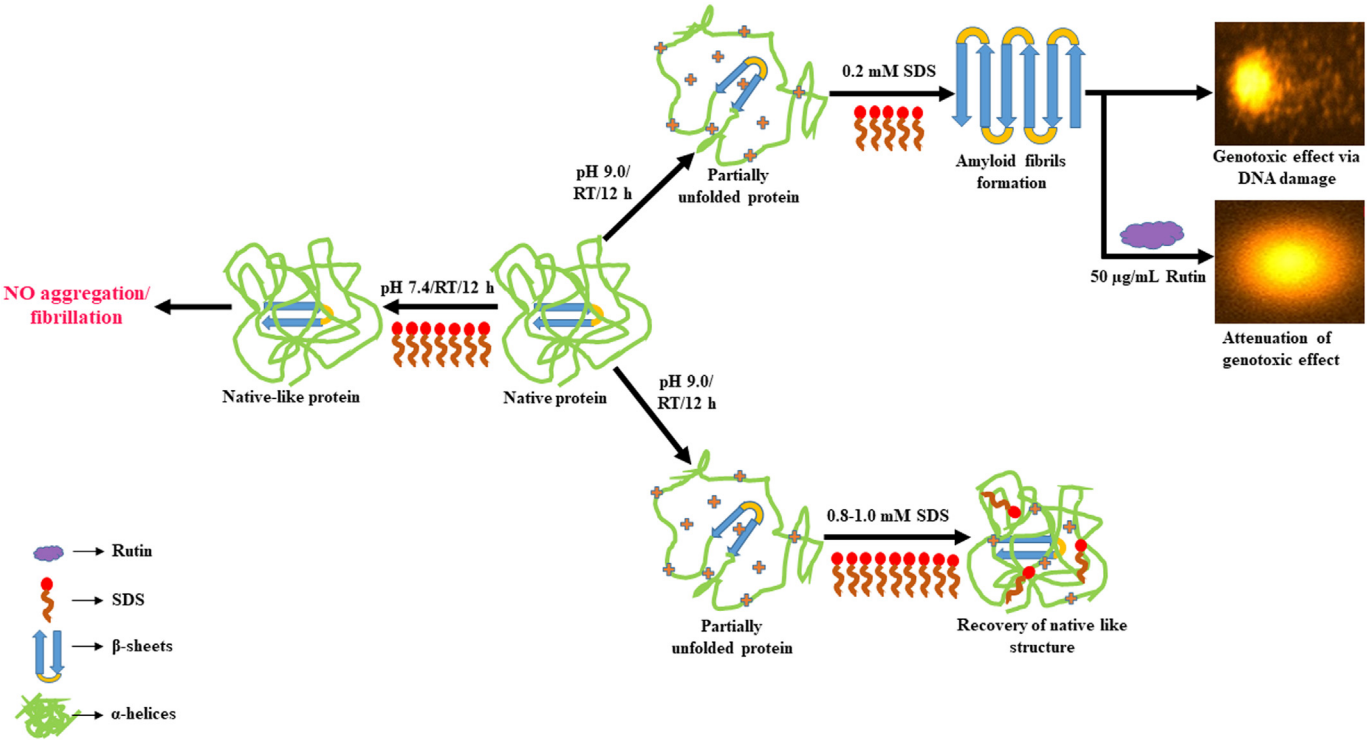

Fig. 14. Mechanistic pathway of lysozyme aggregation and their inhibition by polyphenols (rutin).

pronounced at lower concentrations. Higher concentration of SDS (0.8–1.0 mM) was less than its CMC (8.01 mM) value, thus; the stabilizing effect of SDS might be due to hydrophobic or crowding effect. The CD study indicates a loss in helicity in the presence of SDS. Turbidity assay shows aggregation propensity of HEWL is maximum in the presence of 0.2 mM SDS. The reason behind the inhibition potency of rutin is attributed to a combination of its greater radical scavenging ability along with significant aromatic and hydrophobic interactions. The predicted mechanism for SDS induced lysozyme aggregation and their attenuation are represented in Fig. 14. Further elucidation of structure-activity relations of such inhibitors is required to enhance our knowledge of inhibition of aggregated fibrillar species that play a major role in neurodegenerative diseases.

Supplementary data to this article can be found online at https://doi.org/10.1016/j.ijbiomac.2018.07.112.

Conflict of interest

There is no any conflict of interest between authors.

Acknowledgements

The authors extend their appreciation to the Deanship of Scientific Research at King Saud University, Riyadh, Saudi Arabia for funding this work through research group project number RGP-215.

References

[1] C.A. Ross, M.A. Poirier, Protein aggregation and neurodegenerative disease, Nat. Med. 10 (2004) S10–S17.
[2] M.R. Sawaya, S. Sambashivan, R. Nelson, et al., Atomic structures of amyloid cross-β spines reveal varied steric zippers, Nature 447 (2007) 453–457.
[3] F. Chiti, C.M. Dobson, Protein misfolding, functional amyloid, and human disease, Annu. Rev. Biochem. 75 (2006) 333–366.
[4] J.C. Rochet, P.T. Lansbury Jr., Amyloid fibrillogenesis: themes and variation, Curr. Opin. Struct. Biol. 10 (2000) 60–68.
[5] C.M. Dobson, Protein folding and misfolding, Nature 426 (2003) 884–890.
[6] B. De Meulenaer, B. Kerkaert, F. Mestdagh, Detection of hen's egg white lysozyme in food: comparison between a sensitive HPLC and a commercial ELISA method, Food Chem. 120 (2010) 580–584.
[7] V.A. Proctor, F.E. Cunningham, The chemistry of lysozyme and its use as a food preservative and a pharmaceutical, CRC Crit. Rev. Food Sci. Nutr. 26 (1988) 359–395.
[8] K.A. Bolin, G.L. Millhauser, Alpha and 3(10): the split personality of polypeptide helices, Acc. Chem. Res. 32 (1999) 1027–1033.
[9] M.C. Vaney, S. Maignan, M. RiesKautt, A. Ducruix, High-resolution structure (1.33 angstrom) of a HEW lysozyme tetragonal crystal grown in the APCF apparatus. Data and structural comparison with a crystal grown under microgravity from SpaceHab-01 mission, Acta Crystallogr. D Biol. Crystallogr. 52 (1996) 505–517.
[10] L.A. Morozova-Roche, J. Zurdo, A. Spencer, W. Noppe, V. Receveur, et al., Amyloid fibril formation and seeding by wild-type human lysozyme and its disease-related mutational variants, J. Struct. Biol. 130 (2000) 339–351.
[11] M.R.H. Krebs, D.K. Wilkins, E.W. Chung, M.C. Pitkeathly, A.K. Chamberlain, et al., Formation and seeding of amyloid fibrils from wild-type hen lysozyme and a peptide fragment from the beta-domain, J. Mol. Biol. 300 (2000) 541–549.
[12] M.B. Pepys, P.N. Hawkins, D.R. Booth, D.M. Vigushin, G.A. Tennent, et al., Human lysozyme gene-mutations cause hereditary systemic amyloidosis, Nature 362 (1993) 553–557.
[13] L.N. Arnaudov, R. de Vries, Thermally induced fibrillar aggregation of hen egg white lysozyme, Biophys. J. 88 (2005) 515–526.
[14] S. Goda, K. Takano, Y. Yamagata, R. Nagata, H. Akutsu, et al., Amyloid protofilament formation of hen egg lysozyme in highly concentrated ethanol solution, Protein Sci. 9 (2000) 369–375.
[15] B.A. Vernaglia, J. Huang, E.D. Clark, Guanidine hydrochloride can induce amyloid fibril formation from hen egg-white lysozyme, Biomacromolecules 5 (2004) 1362–1370.
[16] S.S.S. Wang, K.N. Liu, W.H. Lee, Effect of curcumin on the amyloid fibrillogenesis of hen egg-white lysozyme, Biophys. Chem. 144 (2009) 78–87.
[17] H. Yagi, T. Ban, K. Morigaki, H. Naiki, Y. Goto, Visualization and classification of amyloid â supramolecular assemblies, Biochemistry 46 (2007) 15009–15017.
[18] Z.Y. Wang, M.T. Huang, Y.R. Lou, J.G. Xie, K.R. Reuhl, H.L. Newmark, C.T. Ho, C.S. Yang, A.H. Conney, Cancer Res. 54 (1994) 3428–3435.
[19] J.V. Higdon, B. Frei, Tea catechins and polyphenols: health effects, metabolism, and antioxidant functions, Crit. Rev. Food Sci. Nutr. 43 (2003) 89–143.
[20] F. Nanjo, K. Goto, R. Seto, M. Suzuki, M. Sakai, Y. Hara, Scavenging effects of tea catechins and their derivatives on 1,1-diphenyl-2-picrylhydrazyl radical, Free Radic. Biol. Med. 21 (1996) 895–902.
[21] M. Singh, M. Arseneault, T. Sanderson, V. Murthy, C. Ramassamy, Challenges for research on polyphenols from foods in Alzheimer's disease: bioavailability, metabolism, and cellular and molecular mechanisms, J. Agric. Food Chem. 56 (2008) 4855–4873.
[22] D.Q. Tang, Y.Q. Wei, Y.Y. Gao, X.X. Yin, D.Z. Yang, J. Mou, et al., Protective effects of rutin on rat glomerular mesangial cells cultured in high glucose conditions, Phytother. Res. 25 (2011) 1640–1647.
[23] C.H. Wu, M.C. Lin, H.C. Wang, M.Y. Yang, M.J. Jou, C.J. Wang, Rutin inhibits oleic acid induced lipid accumulation via reducing lipogenesis and oxidative stress in hepatocarcinoma cells, J. Food Sci. 76 (2011) T65–T72.
[24] A. Novakovic, L. Gojkovic-Bukarica, M. Peric, D. Nezic, B. Djukanovic, J. Markovic-Lipkovski, et al., The mechanism of endothelium-independent relaxation induced by the wine polyphenol resveratrol in human internal mammary artery, J. Pharmacol. Sci. 101 (2006) 85–90.
[25] S. Lee, S. Suh, S. Kim, Protective effects of the green tea polyphenol (−)-epigallocatechin gallate against hippocampal neuronal damage after transient global ischemia in gerbils, Neurosci. Lett. 287 (2000) 191–194.
[26] S. Chen, J. Gong, F. Liu, U. Mohammed, Naturally occurring polyphenolic antioxidants modulate IgE-mediated mast cell activation, Immunology 100 (2000) 471–480.
[27] F. Pu, K. Mishima, K. Irie, K. Motohashi, Y. Tanaka, K. Orito, et al., Neuroprotective effects of quercetin and rutin on spatial memory impairment in an 8-arm radial maze task and neuronal death induced by repeated cerebral ischemia in rats, J. Pharmacol. Sci. 104 (2007) 329–334.
[28] W. Tongjaroenbuangam, N. Ruksee, P. Chantiratikul, N. Pakdeenarong, W. Kongbuntad, P. Govitrapong, Neuroprotective effects of quercetin, rutin and okra (Ab elmoschus esculentus Linn.) in dexamethasone-treated mice, Neurochem. Int. 59 (2011) 677–685.
[29] S.W. Wang, Y.J. Wang, Y.J. Su, et al., Rutin inhibits β-amyloid aggregation and cytotoxicity, attenuates oxidative stress, and decreases the production of nitric oxide and proinflammatory cytokines, NeuroToxicology 33 (2012) 482–490.
[30] J.M. Khan, A. Qadeer, S.K. Chaturvedi, E. Ahmad, S. Rehman, S. Gourinath, R.H. Khan, SDS can be utilized as an amyloid inducer: a case study on diverse proteins, PLoS One 7 (2012), e29694. .
[31] N. Rabbani, S. Tabrez, B.U. Islam, M.T. Rehman, A.M. Alsenaidy, M.F. Alajmi, R.A. Khan, M.A. Alsenaidy, M.S. Khan, Characterization of colchicine binding with normal and glycated albumin: in-vitro and molecular docking analysis, J. Biomol. Struct. Dyn. (2017)https://doi.org/10.1080/07391102.2017.1389661 [Epub ahead of print].
[32] A. Qadeer, M. Zaman, R.H. Khan, Inhibitory effect of post-micellar SDS concentration on thermal aggregation and activity of papain, Biochem. Mosc. 79 (2014) 785–796.
[33] M. Biancalana, S. Koide, Molecular mechanism of thioflavin-T binding to amyloid fibrils, Biochim. Biophys. Acta, Proteins Proteomics 1804 (2010) 1405–1412.
[34] X. Zhang, X.X. Sun, D. Xue, D.G. Liu, X.Y. Hu, M. Zhao, et al., Conformation-dependent scFv antibodies specifically recognize the oligomers assembled from various amyloids and show colocalization of amyloid fibrils with oligomers in patients with amyloidoses, Biochim. Biophys. Acta 1814 (2011) 1703–1712.
[35] S. Chibber, M. Farhan, I. Hassan, I. Naseem, White light-mediated Cu (II)-5FU interaction augments the chemotherapeutic potential of 5-FU: an in vitro study, Tumour Biol. 32 (5) (2011) 881–892.
[36] M. Renner, M.A. Danielson, J.J. Falke, 27.Kinetic control of Ca(II) signaling: tuning the ion dissociation rates of EF-hand Ca(II) binding sites, Proc. Natl. Acad. Sci. U. S. A. 90 (14) (1993) 6493–6497.
[37] A. Iram, S. Amani, M. Furkan, A. Naeem, Equilibrium studies of cellulose aggregate in presence of ascorbic and boric acid, Int. J. Biol. Macromol. 52 (2013) 286–295.
[38] R. Swaminathan, V.K. Ravi, S. Kumar, M.V. Kumar, N. Chandra, Lysozyme: a model protein for amyloid research, Adv. Protein Chem. Struct. Biol. 84 (2011) 63–111.
[39] A. Matagne, C.M. Dobson, The folding process of hen lysozyme: a perspective of the new "view", Cell. Mol. Life Sci. 54 (1998) 363–371.
[40] L.J. Smith, M.J. Sutcliffe, C. Redfield, C.M. Dobson, Structure of hen lysozyme in solution, J. Mol. Biol. 229 (1993) 930–944.
[41] A. Matagne, M. Jamin, E.W. Chung, C.V. Robinson, S.E. Radford, C.M. Dobson, Thermal unfolding of an intermediate is associated with non-arrhenius kinetics in the folding of hen lysozyme, J. Mol. Biol. 297 (2000) 193–210.
[42] M. Dumoulin, J.R. Kumita, C.M. Dobson, Normal and aberrant biological self-assembly: insights from studies of human lysozyme and its amyloidogenic variants, Acc. Chem. Res. 39 (2006) 603–610.
[43] M.R. Krebs, D.K. Wilkins, E.W. Chung, M.C. Pitkeathly, A.K. Chamberlain, J. Zurdo, C.V. Robinson, C.M. Dobson, Formation and seeding of amyloid fibrils from wildtype hen lysozyme and a peptide fragment from the beta-domain, J. Mol. Biol. 300 (2000) 541–549.
[44] E. Frare, P. Polverino De Laureto, J. Zurdo, C.M. Dobson, A. Fontana, A highly amyloidogenic region of hen lysozyme, J. Mol. Biol. 340 (2004) 1153–1165.
[45] T.A. Pertinhez, M. Bouchard, A.G.R. Smith, C.M. Dobson, J.L. Smith, Stimulation and inhibition of fibril formation by a peptide in the presence of different concentrations of SDS, FEBS Lett. 529 (2002) 193–197.
[46] J. He, Y.F. Xing, B. Huang, Y.Z. Zhang, C.M. Zeng, Tea catechins induce the conversion of preformed lysozyme amyloid fibrils to amorphous aggregates, J. Agric. Food Chem. 57 (2009) 11391–11396.
[47] Grégory F. Schneider, Bryan F. Shaw, Andrew Lee, Emanuel Carillho, George M. Whitesides, Pathway for unfolding of ubiquitin in sodium dodecyl sulfate, studied by capillary electrophoresis, J. Am. Chem. Soc. 130 (51) (2008) 17384–17393.
[48] S. Kumar, A.K. Singh, G. Krishnamoorthy, R. Swaminathan, Thioflavin T displays enhanced fluorescence selectively inside anionic micelles and mammalian cells, J. Fluoresc. 18 (2008) 1199–1205.
[49] P.B. Stathopulos, G.A. Scholz, et al., Sonication of proteins causes formation of aggregates that resemble amyloid, Protein Sci. 13 (2004) 3017–3027.
[50] Y. Porat, A. Abramowitz, E. Gazit, Inhibition of amyloid fibril formation by polyphenols: structural similarity and aromatic interactions as a common inhibition mechanism, Chem. Biol. Drug Des. 67 (1) (2006) 27–37.

[51] M.K. Siddiqi, P. Alam, S.K. Chaturvedi, Saima Nusrat, Y.E. Shahein, R.H. Khan, Attenuation of amyloid fibrillation in presence of warfarin: a biophysical investigation, Int. J. Biol. Macromol. 95 (2017) 713–718.
[52] P. Alam, S.K. Chaturvedi, M.K. Siddiqi, R.K. Rajpoot, M.R. Ajmal, M. Zaman, R.H. Khan, Vitamin k3 inhibits protein aggregation: Implication in the treatment of amyloid diseases, Sci. Rep. 27 (6) (2016) 26759.
[53] P. Alam, M.K. Siddiqi, S.K. Chaturvedi, M. Zaman, R.H. Khan, Vitamin B12 offers neuronal cell protection by inhibiting Aβ-42 amyloid fibrillation, Int. J. Biol. Macromol. 99 (2017) 477–482.
[54] P. Alam, A.Z. Beg, M.K. Siddiqi, S.K. Chaturvedi, R.K. Rajpoot, M.R. Ajmal, M. Zaman, A.S. Abdelhameed, R.H. Khan, Ascorbic acid inhibits human insulin aggregation and protects against amyloid induced cytotoxicity, Arch. Biochem. Biophys. 621 (2017) 54–62.
[55] M.K. Siddiqi, P. Alam, S.K. Chaturvedi, Y.E. Shahein, R.H. Khan, Mechanisms of protein aggregation and inhibition, Front. Biosci. (Elite Ed.) 9 (1–20) (2017).
[56] Y. Tokunaga, Y. Sakakibara, Y. Kamada, K. Watanabe, Y. Sugimoto, Analysis of core region from egg white lysozyme forming amyloid fibrils, Int. J. Biol. Sci. 9 (2) (2013) 219–227.